

The Role of Iodine-123-Tyr-3-Octreotide Scintigraphy in the Staging of Small-Cell Lung Cancer

T. Leitha, S. Meghdadi, M. Studnicka, M. Wolzt, C. Marosi, P. Angelberger, M. Neumann, W. Schlick, K. Kletter and R. Dudczak

University Clinics of Nuclear Medicine and Internal Medicine, Vienna; Chemical Institute, Austrian Research Center Seibersdorf; Center for Pulmonary Diseases, Vienna; and Second University Clinic of Surgery, Vienna, Austria

The purpose of this study is to investigate the role of ^{123}I -Tyr-3-octreotide scintigraphy in staging small-cell lung cancer (SCLC), its efficacy for the discrimination of limited and extensive disease stages and its regional sensitivity for different metastatic locations. Twenty patients with histologically confirmed SCLC and 50 radiologically staged tumor sites were investigated by an imaging protocol including dynamic (0–30 min p.i.), static (30 min, 90 min, 4 hr, 24 hr p.i.) and SPECT (90 min p.i.) studies. The primary tumor site was visualized in 84%, whereas the best delineation was noted in early planar (15–30 min p.i.) and SPECT studies, due to a rapidly decreasing tumor-to-background ratio. Lymph node metastases were seen in 73%, but SPECT was needed for anatomical localization. All three adrenal metastases could be identified in sequential planar images. One clinically unsuspected brain metastasis was seen, whereas a second clinically overt metastasis was not visualized. The global and regional sensitivity for liver and bone metastases was unsatisfactory. In summary, 78% (7/9) of the patients with extensive disease were correctly identified by scintigraphy alone. We conclude that ^{123}I -Tyr-3-octreotide scintigraphy is a substantial tool in the staging work-up of SCLC if it is performed initially to allow fast identification of patients with extensive disease stages and save additional radiological or invasive examinations. Yet, ^{123}I -Tyr-3-octreotide scintigraphy cannot substitute liver sonography or conventional bone scanning in patients who have no scintigraphic evidence of distant tumor spread.

J Nucl Med 1993; 34:1397–1402

Small-cell lung cancer (SCLC) is distinguished from other bronchopulmonary neoplasms by its great likelihood of covert and overt metastatic tumor at diagnosis (1). The clinical performance status and the extent of tumor dissemination are the major prognostic factors (2). Thus, patients

with the histologic or cytologic evidence for SCLC require an extensive and time-consuming staging work-up, including physical examination, chest x-ray, bronchoscopy, CT scan, ultrasound of the upper abdomen, isotope bone scanning and, in certain cases, nuclear magnetic resonance scanning, bone marrow biopsy, mediastinoscopy and diagnostic thoracotomy (3). A clinical two-stage system proposed by the Veterans Administration Lung Cancer Study Group (VALG) (4) distinguishes between limited and extensive disease and has a higher prognostic strength than the commonly used TNM (5) staging system. Any imaging technique capable of discriminating both stages would substantially shorten the time until initiation of therapy.

The radiological staging of mediastinal tumor spread relies on CT scan (6) and nuclear magnetic resonance tomography (7,8). Yet radiological methods are limited by the fact that abnormalities are detected by enlargement and not by visualization of the malignant tissue. Radionuclide imaging methods identify abnormal tissue based on functional changes. However, the staging of lung cancer by ^{67}Ga -citrate scanning is limited by its low specificity (9). A higher specificity of scintigraphy can be obtained by the use of tracers that recognize specific surface antigens of tumor cells (10).

SCLC cells are supposed to stem from amine precursor uptake and decarboxylation (APUD) cells (11,12) and express high affinity somatostatin receptors (13,14). Visualization of somatostatin receptors by ^{123}I -Tyr-3-octreotide scintigraphy has been reported in various tumors (15–17). A recent study (18) has demonstrated imaging of the primary tumor in a small group of patients with SCLC but was not focused on the regional sensitivity of the method.

The purpose of this study is to investigate the role of ^{123}I -Tyr-3-octreotide scintigraphy in staging SCLC, its efficacy for the discrimination of limited and extensive disease stages and its regional sensitivity for different metastatic locations. In addition, the receptor binding characteristics of the tracer should be determined in vivo in order to optimize the imaging protocol for staging SCLC.

Received Dec. 30, 1992; revision accepted Apr. 27, 1993.
For correspondence and reprints contact Thomas Leitha, MD, University Clinic of Nuclear Medicine, University Vienna, Waehringer Guertel 18-20; 1090 Vienna, Austria.

TABLE 1
Patients' Characteristics and Pretreatment

Patients				Primary tumor			Metastases		Pretreatment		
No.	Age	Sex	Stage	Size	Dynamic study 0-30 min p.i.	Static study 30 min p.i.	SPECT study 90 min p.i.	Lymph node localization	Other localizations	Chemo- therapy	Radia- tion
1	58	F	LD	7 cm	±	-	+	Mediastinal	Pulmonal	+	-
2	61	M	ED	10 cm	-	+	+	Mediastinal	Pleural	+	-
3	67	M	LD	4 cm	-	±	+	Hilar		+	+
4	51	M	LD	3 cm	+	+	+	Mediastinal		+	-
5	66	M	LD	3 cm	-	-	-	Hilar		-	-
6	57	M	ED	5 cm	±	+	±	Mediastinal	Both adrenals, brain	+	+
7	65	M	LD	7 cm	±	±	+	Mediastinal	Pulmonal	+	+
8	73	M	ED	6 cm	±	+	±		Adrenals, liver	+	-
9	63	M	LD	6 cm	±	+	±			+	-
10	75	M	LD	6 cm	+	+	+	Mediastinal		+	-
11	58	M	LD	3 cm	-	-	+	Mediastinal		+	+
12	56	M	LD	4 cm	-	-	-	Hilar		+	-
13	89	M	ED	10 cm	+	+	+	Mediastinal	Pulmonal, bone	+	+
14	48	M	ED	5 cm	-	-	-	Hilar	Liver, bone	+	+
15	48	M	LD	10 cm	+	+	+	Mediastinal		+	+
16	61	M	LD	2 cm	+	+	±			+	-
17	65	M	ED	4 cm	+	+	+	Hilar	Pulmonal	+	-
18	62	M	ED	—	-	-	-		Bones	+	+
19	68	M	ED	8 cm	+	+	+	Cervical		+	-
20	48	F	ED	8 cm	+	+	+	Mediastinal	Brain, bone	+	-

Note: Image rating: +, positive; ±, positive in the knowledge of the radiological tumor site; -, negative.

MATERIALS AND METHODS

Patients

Twenty patients (18 male, 2 female, age, 62 ± 10 yr) with histologically confirmed SCLC were studied. All patients gave informed consent to participate in the study protocol, which was approved by the ethical committee of our institution.

The diagnostic work-up included chest x-ray in two planes, bronchoscopy (with biopsy and lavage), thoracic CT scan including the region of the adrenal glands, abdominal sonography and bone scanning within four weeks to ^{123}I -Tyr-3-octreotide scintigraphy. Brain CT scan was performed in cases with clinical or scintigraphic suspicion for brain metastases. Results of the clinical staging are given in Table 1.

Primary tumor size ranged from 2 to 10 cm (median = 3 cm) in 19 patients. One patient (no. 18) had no primary tumor site after pneumectomy. Lymph node metastases ranging from 1 to 5 cm in diameter (median = 3 cm) were found in 15 patients, pleuropulmonary metastases in five (two into the contralateral lung), bone metastases in four, liver metastases in two and brain metastases in two patients, respectively. One patient (no. 6) had bilateral adrenal metastases and one (no. 8) had metastases in the right adrenal gland.

Nine patients had extensive disease, whereas eleven had limited disease according to the clinical and radiological staging. All but one patient had chemotherapy 1-8 wk prior and 8 of 20 patients had radiotherapy 1-18 mo prior to scintigraphy.

Radiopharmaceutical Labeling

Tyr-3-octreotide (SDZ 204-090, Sandoz Basel, Switzerland) was labeled with ^{123}I (Medgenix, Belgium) by the method of Bakker et al. (19). The labeled product was purified by preparative HPLC (RP19) or solid-phase extraction column (C18) chro-

matography. Radiochemical purity was determined by analytical HPLC (RP18). The isolated radiochemical yield was $67\% \pm 8\%$; the radiochemical purity was $>98\%$ and remained stable in vitro for more than 20 hr. The administered dose varied between 296-444 MBq.

Imaging Protocol

Thyroid blocking with potassium iodine was started one day before and continued until the third day after tracer injection. All studies were acquired with a large field of view gamma camera (GCA 901A Toshiba Corp.) and analyzed by the New GMS software (V5.0; Toshiba Corp.).

Dynamic scintigraphy (128×128 matrix; 1 frame/min) was started at the time of tracer injection and continued until 30 min postinjection (p.i.). Static images (128×128 ; 500,000 counts/frame) of the head (anterior, posterior projection), the thorax (anterior, left lateral, posterior, right lateral projection), the abdomen (anterior, posterior projection) and the pelvis, including the upper third of the thigh (anterior, posterior projection), were obtained 30 min, 90 min, 4 hr and 24 hr p.i. Single-photon emission computed tomography (SPECT) of the thorax (128×128 matrix, 60 stops, 360° , 40 sec/stop) was obtained 90 min p.i. in all patients. Transaxial, coronal and sagittal slices were reconstructed after prefiltering (3×3 , normal pass) using a ramp filter. SPECT of other regions were performed in cases with an abnormal planar image of the region.

Digitized images were analyzed by two experienced investigators without the knowledge of the clinical staging. A focal increased tracer accumulation that could not be attributed to the blood pool or the biliary excretion of the tracer was regarded as positive receptor imaging.

Statistical Analysis

Primary tumor site imaging was rated individually for the dynamic, static and SPECT studies in comparison with the clinical staging as scintigraphically positive (+), positive only in the knowledge of the tumor site (\pm) or negative (-). Tumor-to-background ratios were determined in planar images in which the tumor was visualized best by drawing a rectangular region over the tumor and four adjacent background regions. The ratio of counts per pixel over the tumor and the mean of counts per pixel in the background regions were calculated in all patients. In cases without tumor imaging, the ratio was set to 1. Imaging of metastases was rated by a two-scale system as positive, if a true-positive imaging was noted at any imaging time and as negative in all other cases. All results are given as mean \pm s.d. **Information content** of ^{123}I -Tyr-3-octreotide scintigraphy is calculated individually for the detection of the primary tumor site and the main metastatic sites. **Sensitivity** is the number of patients with a true positive scintigraphic result divided by the total number of patients with clinical evidence for tumor tissue according to the results of the clinical staging. **Specificity** is the number of patients with true-negative scintigraphic results divided by the total number of patients without clinical evidence for tumor tissue. **Accuracy** is determined by the number of patients with true-positive or true-negative scintigraphic results divided by the total number of patients investigated. **Positive predictive value** is the number of patients with true-positive scintigraphic results divided by the number of patients with true-positive or false-positive scintigraphic results. **Negative predictive value** is the number of patients with true-negative scintigraphic results divided by the number of patients with true-negative or false-negative scintigraphic results.

RESULTS

All patients tolerated tracer injection without side effects and all studies were obtained according to the imaging protocol.

The information content of dynamic (0–30 min p.i.) early planar (30 min p.i.) and SPECT (90 min p.i.) studies for primary tumor site imaging is shown in Table 1. The lower number of (+) and the higher number of (\pm) results in the dynamic studies appears to be caused in part by centrally located tumors that could not be clearly separated from the mediastinal blood pool. The primary tumor site was imaged best in the early planar images (dynamic and static studies 15–30 min p.i.) (Fig. 1) and in SPECT. Both were comparable in the number of (+) results, but a higher number of positive tumor images was noted in SPECT if the information of the radiologically determined tumor localization was available (\pm results). However, the optimal imaging time and study type was different for each primary tumor; thus 16 of 19 tumors were at least positive (+) in one study, thus accounting for a sensitivity of 84%. This may be explained in part by a rapidly decreasing tumor-to-background contrast (30 min p.i.: 1.2 ± 0.3 ; 90 min p.i.: 1.1 ± 0.1 ; 4 hr p.i.: 1.1 ± 0.1 ; 24 hr p.i.: 1.0 ± 0.0 ; n = 19 primary tumors), which compromised the higher contrast obtained by SPECT by a lower tracer uptake of the target at later imaging time points. Preceding radiotherapy or chemotherapy had no evident effect on imaging results as one of the

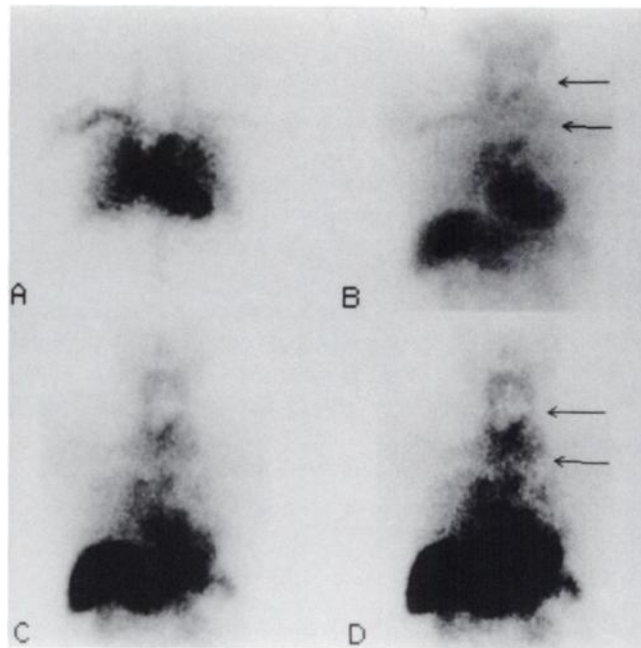


FIGURE 1. Early ^{123}I -Tyr-3-octreotide accumulation in SCLC tissues. Images A–C are part of the dynamic study; image D is the early static study of Pat. No. 19. Image A shows blood pool activity 0–2 min after tracer injection. Image B shows a faint tracer accumulation in the cervical lymph node metastasis (left paramedian, 8 cm diameter; arrows), 8–10 min p.i. The primary tumor in the trachea is masked by blood pool activity of large vessels. Image C shows a definite tracer accumulation in the cervical lymph node metastasis, 18–20 min p.i. The highest tracer uptake is noted in the cranial parts, due to necrosis and diminished blood flow in the center of the lymph node. Image D is part of the static study 30 min p.i. and reproduces the positive imaging of the lymph node metastasis (arrows).

patients with negative tumor imaging had no preceding therapy, one had chemotherapy only and one had combined radiotherapy and chemotherapy. In contrast, five patients with combined therapy had positive tumor imaging. As none of the patients in our study had an abnormal lung architecture (e.g., atelectases, pleural effusion), the scintigraphically determined tumor dimensions were comparable to the results of radiological methods.

Positive imaging of radiologically suspected lymph node metastases was noted in 73% of patients. The high blood-pool activity masked positive imaging of mediastinal lymph nodes in the dynamic studies. The majority of the positive lymph nodes was suspected in early planar images, but an anatomical localization SPECT scan was needed (Fig. 2).

All three sites of adrenal metastases were visualized in planar studies, but the interpretation was substantially impaired by a high initial tracer uptake into the liver and later by the biliary excreted activity into the intestines. Moreover, due to the high activity content of the gallbladder, SPECT images of the upper abdomen were hampered by reconstruction artifacts. The diagnosis of adrenal metastases was thus based on comparison of initial and late posterior planar images, whereas a fixed-activity uptake was regarded as a positive image. The high liver uptake and the

biliary tracer excretion masked a possible imaging of liver metastases in all patients. The sensitivity for bone metastases was 50%, because skeletal metastases were identified only in two of four patients. However, the number of metastases was underestimated in both patients. The sensitivity for pleuropulmonary metastases was 40%. It is noteworthy that both patients with metastases into the contralateral lung were identified, but metastases in the homolateral lung were scintigraphically negative. One patient with an unsuspected brain metastasis was identified with SPECT (Fig. 3), whereas a second patient with clinically overt brain metastases was missed. Table 2 provides ^{123}I -Tyr-3-octreotide scintigraphy data for different tumor sites.

In summary, seven of nine (78%) patients with extensive disease were correctly identified by ^{123}I -Tyr-3-octreotide scintigraphy.

DISCUSSION

The efficacy of ^{123}I -Tyr-3-octreotide scintigraphy for staging SCLC was investigated in comparison with results of radiological staging in 20 patients with 50 tumor sites. The primary tumor was identified in 84% of patients. The sensitivity of ^{123}I -Tyr-3-octreotide scintigraphy in our study appeared to be higher than previously reported in a smaller group of patients (18). This may be due to a higher number of early imaging points in the protocol. However, the tumor-to-background contrast was low and decreased

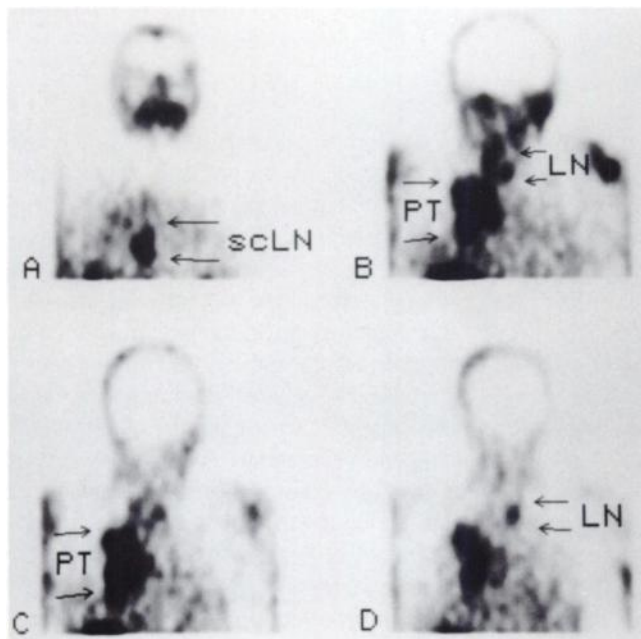
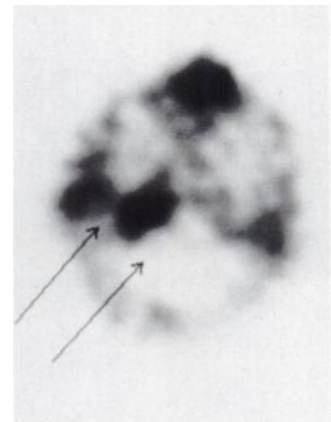


FIGURE 2. Anatomical localization of ^{123}I -Tyr-3-octreotide accumulation in SPECT. The coronal SPECT images of the head and thorax (Pat. No. 20) show positive image of the primary tumor and lymph node metastases. The subcarinal lymph node metastasis (scLN) is seen in Image A. The primary tumor (PT, diameter 8 cm) in the right upper lung lobe is delineated best in Images B and C. Lymph node metastases (LN) in the superior mediastinum are best seen in Images B, C and D. Increased activity in the lower left part of all images represents physiological tracer uptake by the liver.

FIGURE 3. Iodine-123-Tyr-3-octreotide imaging of a clinically unsuspected brain metastasis in SPECT. The transaxial SPECT image of the head (Pat. No. 20) shows positive image of a clinically unsuspected brain metastasis. The parietobasal activity accumulation on the right was not seen on planar images but could be clearly delineated in SPECT.



rapidly in spite of a fast blood clearance of the tracer (20); thus a transitory receptor-binding of the tracer has to be assumed. This also has been considered by Kwekkeboom et al. (18), who described fugitive imaging of SCLC, but unfortunately have not quantitated the time course of tumor contrast in their study. The rapidly decreasing tracer accumulation may suggest a certain extent of unspecific uptake; however, the visible ^{123}I -Tyr-3-octreotide accumulation outlasts blood-pool activity by far, and imaging of hypervascular tumor spots thus seems unlikely as the primary mechanism of uptake.

The optimal imaging time for the primary tumor in our study was 15–30 min p.i., which is in line with observations by others (21,22) who have reported early imaging of somatostatin receptors in several tumors. Of note is that preceding chemotherapy and radiotherapy seemed to have no striking effect on receptor imaging. This is in agreement with Brambilla et al. (23), who found stable neuroendocrine linkage markers in spite of multidirectional phenotypic changes in SCLC after chemotherapy. Thus, ^{123}I -Tyr-3-octreotide scintigraphy could be useful for detecting tumor recurrence after therapy, although this has to be confirmed in future longitudinal studies. The sensitivity of ^{123}I -Tyr-3-octreotide scintigraphy for radiologically confirmed metastases in intrathoracic and extrathoracic lymph nodes is of outstanding importance for the discrimination of limited and extensive disease stages. In our experience, 73% of known lymph node metastases could be visualized by scintigraphy. Involvement of mediastinal lymph nodes was often suspected in early planar images, but in most cases SPECT 90 min p.i. was necessary for anatomical localization. Earlier SPECT imaging may have been advantageous because of higher tracer uptake, but dynamic SPECT with a two-head or three-head gamma camera device would have been needed to account for the rapidly changing activity distribution early after tracer injection.

SCLC is characterized by early metastases to the adrenal glands (24). CT scanning of the upper abdomen is customary for radiological staging of lung cancer, but the high prevalence of nonmalignant enlargements of adrenals

TABLE 2
Information Content of Staging SCLC with ¹²³I-Tyr-3-octreotide Scintigraphy

Tumor Sites	Statistics				
	Sensitivity	Specificity	Accuracy	PPV	NPV
Primary tumor	16/19 (84)	1/1 (100)	17/20 (85)	16/16 (100)	1/4 (25)
Metastases					
Lymph nodes	11/15 (73)	5/5 (100)	16/20 (80)	11/11 (100)	5/9 (56)
Pleuropulmonary	2/5 (40)	15/15 (100)	17/20 (85)	2/2 (100)	15/18 (83)
Bones	2/4 (50)	16/16 (100)	18/20 (90)	2/2 (100)	16/18 (89)
Liver	0/2 (0)	18/18 (100)	18/20 (90)	—	18/20 (90)
Adrenal glands	2/2 (100)	18/18 (100)	20/20 (100)	2/2 (100)	18/18 (100)
Brain	1/2 (50)	18/18 (100)	19/20 (95)	1/1 (100)	18/19 (95)
Staging of extensive disease	7/9 (78)	11/11 (100)	18/20 (90)	7/7 (100)	11/13 (85)

Note: All table values are number of patients; the values within parentheses are percentages. PPV = positive predictive value; NPV = negative predictive value.

hampers CT specificity, may overestimate tumor spread and may prevent the patient from having potentially curative surgery. Iodine-123-Tyr-3-octreotide scintigraphy visualized all three sites of adrenal metastases in two patients. However, the unspecific biliary and intestinal tracer accumulation made diagnosis difficult because it hampered SPECT reconstruction and masked specific uptake in the adrenals. Yet, a specific uptake in the adrenals could be delineated up to 24 hr p.i. Imaging results with ¹²³I-Tyr-3-octreotide scintigraphy were disappointing in both locations. Neither of the two patients with sonographically diagnosed liver metastases could be identified by scintigraphy. The high physiological tracer uptake and the rapid biliary excretion masked a possible tumor identification. The higher contrast of SPECT could not be used because of reconstruction artifacts caused by focal activity in the gallbladder. Bone metastases were seen in two of four patients, but the number of metastases was underestimated in comparison with conventional bone scanning. Our data do not provide any explanation for this poor sensitivity of ¹²³I-Tyr-3-octreotide scintigraphy in the bone, but reduced blood flow or lower receptor expression may be possible causes.

Iodine-123-Tyr-3-octreotide scintigraphy was useful in screening for brain metastases, because one unsuspected brain metastasis was found with SPECT that could later be confirmed by CT. Yet, one patient with brain metastases was missed. In summary, ¹²³I-Tyr-3-octreotide scintigraphy did not identify lesions that would have been missed by extended conventional staging, but as a single investigation, it was able to identify 78% of patients with extensive disease.

The features of ¹²³I-Tyr-3-octreotide scintigraphy are best used if performed as the initial step in staging SCLC patients. It has a high positive and negative predictive value for identifying extensive disease stages and thus allows identification of the majority of patients. For those patients, further staging procedures and surgery can be omitted and chemotherapy is not further delayed. In view of our results of rapidly decreasing tumor contrast and

tumor sites visible no later than 90 min p.i., a short imaging protocol is favored. We recommend dynamic imaging over the thorax until 30 min p.i., followed by a whole-body scan and SPECT of the head and mediastinum. Later planar imaging may be necessary for differential diagnosis of specific uptake of adrenal metastases and unspecific intestinal activity.

In summary, ¹²³I-Tyr-3-octreotide scintigraphy is a substantial tool in SCLC, if performed as the initial step in the staging work-up to allow fast identification of patients with extensive disease and save additional examinations. It cannot, however, substitute for liver sonography or conventional bone scanning to screen liver and bone metastases in patients with no scintigraphic evidence of distant tumor spread.

REFERENCES

1. Matthews MJ, Kanhouwa S, Picker J, et al. Frequency of residual and metastatic tumors in patients undergoing curative surgical resection of lung cancer. *Cancer Chemother Rep* 1973;3:63-67.
2. Stahel RA, Ginsberg R, Havemann K, et al. Staging and prognostic factors in small cell lung cancer: a consensus report. *Lung Cancer* 1989;5:119-126.
3. Aissner J, Whitley NO. Current staging of lung cancer: an overview of current and newer approaches. In: Hansen HH, ed. *Basic and clinical concepts of lung cancer*. Boston: Kluwer Academic; 1989: 183-213.
4. Zelen M. Keynote address on biostatistics and data retrieval. *Cancer Chemother Rep* 1973;3/4:31-42.
5. Mountain CF. A new international staging system for lung cancer. *Chest* 1986;89:225-233.
6. Spiro SG, Goldstraw T. The staging of lung cancer. *Thorax* 1985;39:401-407.
7. Poon PY, Bronskill MJ, Henkelman M, et al. Mediastinal lymph node metastases from bronchogenic carcinoma: detection with MR imaging and CT. *Radiology* 1987;162:651-656.
8. Jelinek JS, Redmond J, Perry JJ, et al. Small cell lung cancer: staging with MR imaging. *Radiology* 1990;177:837-842.
9. McKenna RJ, Haynie TP, Libshitz HI, Mountain CF, McMurtrey MJ. Critical evaluation of the gallium-67 scan for surgical patients with lung cancer. *Chest* 1985;87:428-431.
10. Leitha T, Walter R, Schlick W, Dudczak R. Tc-99m anti-CEA radioimmunosintigraphy of lung adenocarcinoma. *Chest* 1991;99:14-19.
11. Baylin SB, Jackson RD, Goodwin G, Gazdar AF. Neuroendocrine-related biochemistry in the spectrum of human lung cancer. *Exp Lung Res* 1982;3: 209-223.
12. Gazdar AF, Carney DN, Russell EK, et al. Establishment of continuous, clonable cultures of small-cell carcinoma of the lung which have amine

- precursor uptake and decarboxylation cell properties. *Cancer Res* 1980;40:3502-3507.
13. Reubi JC, Waser B, Sheppard M, Macaulay V. Somatostatin receptors are present in small-cell but not in non-small-cell primary lung carcinomas: relationship to EGF receptors. *Int J Cancer* 1990;45:269-274.
 14. Taylor JE, Coy DH, Moreau JP. High affinity binding of (I-125-Tyr-11) somatostatin-14 to human small-cell lung carcinoma (NCI-H69). *Life Sci* 1988;43:421-427.
 15. Krenning EP, Bakker WH, Breeman WAP, et al. Localisation of endocrine-related tumours with radioiodinated analogue of somatostatin. *Lancet* 1989; i:242-244.
 16. Lamberts SWJ, Hofland LJ, van Koetsveld P, Reubi JC, Bakker WH, Krenning EP. Parallel in vivo and in vitro detection of functional somatostatin receptors in human endocrine pancreatic tumors. Clinical consequences with regard to medical therapy. *J Clin Endocrinol Metab* 1990;71:566-574.
 17. Bakker WH, Krenning EP, Breeman WA, et al. Receptor scintigraphy with a radioiodinated somatostatin analogue: radiolabeling, purification, biological activity and in vivo application in animals. *J Nucl Med* 1990;31:1501-1509.
 18. Kwekkeboom DJ, Krenning EP, Bakker WH, et al. Radioiodinated somatostatin analog scintigraphy in small-cell lung cancer. *J Nucl Med* 1991;32:1845-1848.
 19. Bakker WH, Krenning EP, Breeman WA, et al. Receptor scintigraphy with a radioiodinated somatostatin analogue: radiolabeling, purification, biological activity and in vivo application in animals. *J Nucl Med* 1990;31:1501-1509.
 20. Krenning EP, Bakker WH, Kooji PPM, et al. Somatostatin receptor scintigraphy with indium-111-DTPA-D-Phe-1-octreotide in man: metabolism, dosimetry and comparison with iodine-123-Tyr-3-octreotide. *J Nucl Med* 1992;33:652-658.
 21. Lamberts SWJ, Bakker WH, Reubi JC, Krenning EP. Somatostatin-receptor imaging of endocrine tumors. *N Engl J Med* 1990;323:1246-1249.
 22. Bakker WH, Krenning EP, Breeman WA, et al. In vivo use of a radioiodinated somatostatin analogue: dynamics, metabolism and binding to somatostatin receptor-positive tumors in man. *J Nucl Med* 1991;32:1184-1189.
 23. Brambilla E, Moro D, Gazzeri S, et al. Cytotoxic chemotherapy induces cell differentiation in small-cell lung carcinoma. *J Clin Oncol* 1991;9:50-61.
 24. Matthews MJ. Problems in morphology and behavior of bronchopulmonary malignant disease. In: Israel L, Chahanian P, eds. *Lung cancer: natural history. Prognosis and therapy*. New York: Academic Press; 1976:23-62.